https://doi.org/10.17221/161/2023-HORTSCI

Identification and validation of stem rot disease resistance genes in passion fruit (*Passiflora edulis*)

Yanyan Wu[1], Guoying Shi[2], Junniu Zhou[1], Qinglan Tian[1], Jieyun Liu[1], Weihua Huang[1], Xiuzhong Xia[3], Haifei Mou[1]*, Xinghai Yang[3]**

[1]*Biotechnology Research Institute, Guangxi Academy of Agricultural Sciences, Nanning, P.R. China*
[2]*Microbiology Research Institute, Guangxi Academy of Agricultural Sciences, Nanning, P.R. China*
[3]*Rice Research Institute, Guangxi Key Laboratory of Rice Genetics and Breeding, Guangxi Academy of Agricultural Sciences, Nanning, P.R. China*

**Corresponding authors: xiaxiuzhong@163.com; mhf@gxaas.net; yangxinghai514@163.com*

Yanyan Wu and Guoying Shi contributed equally to this work.

Citation: Wu Y., Shi G., Zhou J., Tian Q., Liu J., Huang W., Xia X., Mou H., Yang X. (2025): Identification and validation of stem rot disease resistance genes in passion fruit (*Passiflora edulis*). Hort. Sci. (Prague), 52: 67–80.

Abstract: Stem rot disease poses a significant challenge in passion fruit production, necessitating the identification of resistant genes for the development of stem rot resistant varieties. In this study, we conducted artificial inoculation of *Fusarium solani* on leaves of two passion fruit varieties, 'Huangjinguo' and 'Ziguo 7'. Leaf samples were collected at 0 h, 24 h, and 48 h post-inoculation for RNA-sequencing (RNA-seq) analysis, and 3 370, 4 464, and 3 974 differentially expressed genes (DEGs) were identified at these stages. Gene Ontology (GO) analysis revealed associations with functions such as response to reactive oxygen species (ROS), response to hydrogen peroxide, and protein complex oligomerisation. Kyoto Encyclopedia of Genes and Genomes (KEGG) analysis highlighted the enrichment of DEGs in the phenylpropanoid biosynthesis pathway, including genes such as *ZX.06G0025070*, *ZX.01G0064640*, *ZX.04G0011040*, *ZX.05G0011380*, all implicated in lignin biosynthesis. Weighted gene co-expression network analysis (WGCNA) identified three modules significantly associated with passion fruit stem rot resistance. Network analysis highlighted *ZX.08G0013660* as the gene with the highest connectivity in these modules, featuring a leucine-rich repeat domain. Reverse transcription quantitative real-time polymerase chain reaction (RT-qPCR) analysis further validated *ZX.08G0013660* and other genes as potential candidates for passion fruit stem rot resistance. Overall, genes related to ROS, phenylpropanoid biosynthesis and leucine-rich repeat domain protein likely play critical roles in passion fruit stem rot resistance. This study provides new insights for breeding passion fruit varieties resistant to stem rot disease.

Keywords: candidate genes; disease resistance; *Fusarium solani*; Huangjinguo; RNA-sequencing; WGCNA

Supported by the National Natural Science Foundation of China (Grant No. 32060660 and 32260740), Guangxi Natural Science Foundation of China (Grant No. 2023GXNSFAA026301), Guangxi Ministry of Science and Technology (Grant No. GuikeAA22068091-1) and Guangxi Academy of Agricultural Sciences (Grant No. 2021YT089).

https://doi.org/10.17221/161/2023-HORTSCI

Cultivated passion fruit is a vital fruit tree in southern China. As an herbaceous vine plant, passion fruit yields aromatic fruits abundant in sugars, vitamins, calcium, iron, zinc, and other essential minerals, making it highly nutritious. With the improvement of living standards and changes in consumer preferences in China, there has been a rapid increase in passion fruit consumption, driving the rapid expansion of the passion fruit industry. However, the occurrence and dissemination of passion fruit stem rot disease caused by fungi such as *Fusarium oxysporum* and *Fusarium solani* pose a serious threat to passion fruit yield and quality.

To date, researchers have identified some stem rot resistance genes/QTLs (quantitative trait loci) in various plants, such as soybeans (Du et al. 2018), sorghum (Funnell-Harris et al. 2019), and maise (Chen et al. 2017; Ma et al. 2017; Duan et al. 2019), with more in-depth studies on maise stem rot-related genes (Belisário et al. 2022). Ye et al. (2013) investigated the functionality of QTL *qRfg1* in maise, observing its response to *Fusarium graminearum*, suggesting its role as a transcription factor responsive to various abiotic stresses. Subsequently, Liu et al. (2016) used RNA-sequencing (RNA-seq) analysis to discover that *qRfg1* induces defence-related genes, while *qRfg2* enhances maise resistance to stalk rot through alleviating auxin signalling transduction and inhibiting auxin polar transport. Furthermore, Wang et al. (2017a) finely mapped the major QTL *qRfg1* for maise resistance to *Fusarium graminearum* stalk rot to a region of approximately 170 kb. They identified *ZmCCT* as a candidate gene, which belongs to the *CCT* gene family and plays a crucial role in plant-specific responses to external environmental signals. Recently, Ye et al. (2019) precisely located the maise QTL *qRfg2* for *Fusarium* stalk rot resistance within a 2.6-kb interval. The candidate gene *GRMZM2G063298* (*ZmAuxRP1*) encodes an auxin-regulated protein, which rapidly responds to pathogen attacks, leading to inhibited root growth but enhanced resistance to *Fusarium* stalk rot. Bai et al. (2021) identified the transcription factor ZmWRKY83 and validated its function in maise stalk rot resistance. Furthermore, Du et al. (2023) fine-mapped *qPss3* on maise chromosome 3, conferring high resistance to stalk rot. Ma et al. (2023) discovered *ZmWAX2* as a candidate gene through a genome-wide association study, enhancing resistance to seedling blight and stalk rot in maise. These findings indicate the presence of genes influencing resistance to stalk rot in plants, providing crucial reference information for identifying genes related to stem rot resistance in cultivated passion fruit varieties.

To date, no reports have documented genes conferring resistance to stem rot disease in passion fruit. In this study, we selected the stem rot-resistant variety 'Huangjinguo' and the susceptible variety 'Ziguo 7' as experimental materials. Through artificial inoculation with *Fusarium solani* and employing RNA-seq technology, we aim to identify genes related to stem rot disease in passion fruit and provide a molecular breeding basis for enhancing passion fruit's resistance to stem rot disease.

MATERIAL AND METHODS

Material planting. In the previous study, we selected the material 'Huangguoyuanshengzhong', which is resistant to stem rot, and the material 'Jinlingziguo', which is susceptible to the disease (Wu et al. 2020). Subsequently, we evaluated the resistance to stem rot disease in the offspring of 'Huangguoyuanshengzhong' seedlings, resulting in the development of the resistant variety 'Huangjinguo'. We used 'Tainong 1' (female parent) to cross with 'Jinlingziguo' (male parent). The offspring bred the excellent variety 'Ziguo 7', but this variety was not resistant to stem rot disease. The experimental materials, 'Huangjinguo' (H) and 'Ziguo 7' (Z), were propagated through cuttings and planted in nutrient cups. At the 8–10 leaf stage, vigorously growing plants with sturdy stems were selected for inoculation with *Fusarium solani*.

***In vivo* inoculation.** The fresh lesion (at the junction of the diseased and healthy areas) tissue block was soaked in 75% ethanol for 30 s and then transferred to 0.1% mercury dichloride for 3 minutes. Then, it was rinsed with sterile water three times, and the surface water was absorbed with sterile filter paper. Subsequently, the tissue block was placed on a separation medium [PDA (potato dextrose agar) containing 150 mg/L streptomycin sulphate] plate and incubated in darkness at 28 °C. The representative strain was obtained after purification of the pathogen isolate.

Live branches and leaves of thymus fruit seedlings, which have been transplanted for 4 months and have been cultivated in the greenhouse, were inoculated with needle and non-invasive inoculation. PDA block culture medium served as the blank control.

https://doi.org/10.17221/161/2023-HORTSCI

Following surface disinfection of the branches with 75% ethanol, the activated strains under constant temperature conditions of 28 °C were made into 5 mm diameter bacterial cakes using a punch and inoculated onto the wounds of the branches. Then, moist and sterile absorbent cotton and cling film were wrapped around the wounds for moisturising. Each treatment was followed by three healthy plants, with three inoculation points for each plant, using sterile PDA blocks as the control. After 48 h, remove the absorbent cotton and observe and record the incidence of the disease. After the symptoms appeared, samples were resampled, isolated, and purified from the lesion. Leaves were collected at 0 h, 24 h, and 48 h after inoculation, quickly frozen in liquid nitrogen, and transferred to a −80 °C refrigerator for storage.

Evaluation of resistance to stem rot disease. Referring to the identification method for resistance to bacterial stripe disease in plants, the grading of the stem rot disease of passion fruit is determined based on the expansion of the disease spots: level 0, no disease spots on the leaves, exhibiting immunity (IM); the ratio of lesions to leaf area is ≤ 1%, high resistance (HR); the ratio of lesions to leaf area between 1–5%: resistance (R); the proportion of lesions to leaf area between 5–25%, moderate susceptibility (MS); the ratio of disease spots to leaf area between 25–50%, infection (S); the ratio of disease spots to leaf area greater than 50%, with leaves wilting and dying, high sensitivity (HS).

mRNA extraction. Total RNA was extracted using the TRIzol® Reagent kit (Invitrogen, USA), following the specific protocol outlined in the user manual. mRNA was enriched using oligo(dT), followed by mRNA fragmentation, cDNA synthesis, and adaptor ligation, following the previously published protocol (Wu et al. 2021).

Transcriptome sequencing. In this study, transcriptome sequencing of passion fruit was conducted using the Illumina NovaSeq 6000 sequencing platform (Illumina, USA). An Illumina PE library was constructed for 2 × 150 bp sequencing, and fastp software version 0.19.5 was used to perform quality control on the obtained sequencing data, including assessing base error rate distribution statistics and evaluating base content distribution. The original data, after quality control, the clean data (reads), was compared with the reference genome using Hisat2 software version 2.1.0. The reference genome source is https://db.cngb.org/search/assembly/CNA0017758/(October 9, 2022). Subsequently, mapped reads were obtained, and RSeQC version 2.3.6 software was used to evaluate the quality of the transcriptome sequencing comparison results, including assessing sequencing saturation, gene coverage, distribution of reads in different regions of the reference genome, and the distribution of reads in different chromosomes. StringTie software version 2.1.2 was used to splice each sample and finally merge them together.

Gene annotation. On October 9, 2022, all genes and transcripts obtained from the transcriptome assembly were aligned in the NR (https://www.ncbi.nlm.nih.gov/public/), Swiss-Prot (http://web.expasy.org/docs/swiss-prot_guideline.html), Pfam (http://pfam.xfam.org/), EggNOG (http://www.ncbi.nlm.nih.gov/COG/), GO (http://www.geneontology.org), and KEGG (http://www.genome.jp/kegg/) databases. This comprehensive comparison aimed to acquire functional information on genes and transcripts, and the annotation status in each database was systematically summarised.

Differentially expressed genes (DEGs) analysis. The overall expression levels of genes/transcripts were quantitatively analysed using the RSEM software (version 1.3.3, http://deweylab.github.io/RSEM/). This analysis aimed to facilitate subsequent examination of differential gene/transcript expression between different samples. The quantitative metric used was TPM (transcripts per million). After obtaining read counts for gene expression analysis, DESeq2 version 1.24.0 was employed for differential expression analysis between samples or groups in the multi-sample project. DEGs/transcripts were identified with the following parameters: P adjust < 0.05 and $|\log_2 FC| \geq 1$.

Gene Ontology (GO) enrichment analysis. The Goatools software version 0.6.5 was used to conduct GO enrichment analysis on the genes within the gene set, aiming to identify the primary GO functions associated with this gene set. The analysis utilised the Fisher's exact test, and a GO function was considered significantly enriched when the adjusted P-value (P adjust) was < 0.05 after correction.

Kyoto Encyclopedia of Genes and Genomes (KEGG) pathway enrichment analysis. R package was used to perform KEGG pathway enrichment analysis on the genes/transcripts within the gene set. The calculation principle was similar to GO functional enrichment analysis, where a KEGG pathway function was considered significantly enriched

https://doi.org/10.17221/161/2023-HORTSCI

when the adjusted *P*-value (*P* adjust) was < 0.05 after correction.

Weighted gene co-expression network analysis (WGCNA). The WGCNA version 1.63 in R package was used to construct a weighted gene co-expression network, with the gene expression profile matrix based on DEGs across all samples. Prior to analysis, the data underwent preprocessing by filtering out genes with low expression (TPM < 1) or small variance (< 0.1). The analysis was conducted using the filtered data. To achieve a scale-free network, the function pickSoftThreshold was employed to calculate weights, and a soft threshold of β = 7 was selected. The dynamic tree-cutting method was then used to obtain hierarchical clustering, with parameters set as minModuleSize = 30, minKMEtoStay = 0.3, and mergeCutHeight = 0.25. The correlation between stem rot disease and modules was calculated to identify key modules. For each gene in the key modules, module membership (MM) and gene significance (GS) values were computed. Genes with high MM and GS values are more likely to be crucial genes. Visualisation analysis was conducted using Cytoscape version 3.8.0 software.

Reverse transcription quantitative real-time polymerase chain reaction (RT-qPCR). *EF-1α-2* (Wu et al. 2020) and *EF1* (Zhao et al. 2022) were used as the reference gene. The expression of *EF-1α-2* and *EF1* was evaluated, and one was selected as the reference gene for this study. RT-qPCR was employed to validate the candidate genes. The specific procedures for RT-qPCR can be found in the previous study (Wu et al. 2021).

Statistical analysis. Excel 2019 and Origin 2019B were used for data statistics. Python software sklear package was used for principal component analysis (PCA). CorelDRAW X8 was used for drawing. Primers were designed using Primer 5 software.

RESULTS

The sequencing quality of 18 samples. After inoculation with *Fusarium solani*, we measured the size of the disease spots 2 days later and took photos (Figure 1). The ratio of disease spots to leaf area in 'Huangjinguo' and 'Ziguo 7' was 1.3% and 31.7%, respectively, indicating R (resistance) and S (susceptibility). Passion fruit leaves were collected at 0 h, 24 h, and 48 h after inoculation with *Fusarium solani*. A total of 18 samples were sequenced using

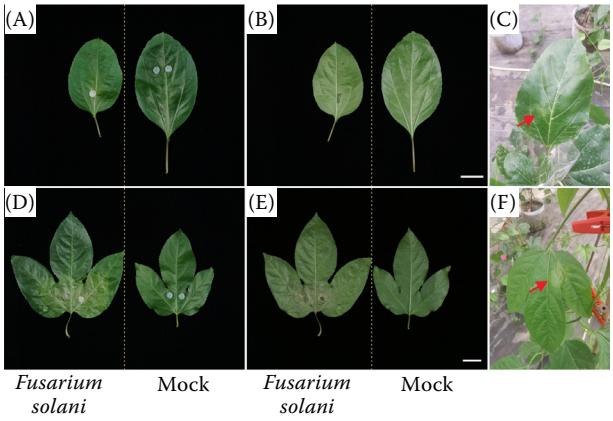

Figure 1. Phenotypes of 'Huangjinguo' and 'Ziguo 7' after 48 h of *Fusarium solani* infection
Scale bars – 3 cm; A, B, C – 'Huangjinguo'; D, E, F – 'Ziguo 7'

the Illumina NovaSeq 6000 sequencer. The clean reads ranged from 44 195 576 to 63 491 736, with an average of 55 083 136. Clean bases ranged from 6 520 913 549 bp to 9 326 950 039 bp, with an average of 8 083 593 249 bp. Quality assessment of the post-quality control sequencing data showed that bases with a sequencing quality above 99.9% (Q30) accounted for 93.9% to 94.6% of the total bases, with an average of 94.3%, exceeding the criterion 80% (Table 1).

Comparison with passion fruit reference genome. The quality-controlled clean data were aligned to the passion fruit reference genome (https://db.cngb.org/search/assembly/CNA0017758/). The number of clean reads mapped to the genome ranged from 23 854 782 to 48 391 337, with a mapping rate of 40.91% to 79.11%, and an average mapping rate of 64.68%. For reads with multiple mapping positions on the reference sequence, the count ranged from 1 133 883 to 3 816 668. Clean reads with a unique mapping position on the reference sequence ranged from 22 720 899 to 45 917 196 [Table S1 in electronic supplementary material (ESM)].

Assembly and annotation. The StringTie software version 2.1.2 was used for reference-based assembly, and the final assemblies were merged together. Comparison with known transcripts allowed the identification of novel transcripts, and functional annotations were performed on these newly identified transcripts. All genes and transcripts obtained from the transcriptome assembly were aligned with NR, Swiss-Prot, Pfam, EggNOG, GO, and KEGG databases to comprehensively obtain functional information on genes and transcripts. A total of 31 809 expressed genes were detected across the 18 sam-

https://doi.org/10.17221/161/2023-HORTSCI

Table 1. Statistics of the transcriptome sequencing data

Sample	Raw reads	Raw bases (bp)	Clean reads	Clean bases (bp)	Error rate (%)	Q20 (%)	Q30 (%)	GC content (%)
Z_A1_1	56 560 658	8 540 659 358	56 069 642	8 216 914 281	0.0245	98.30	94.65	46.40
Z_A1_2	57 509 326	8 683 908 226	56 784 998	8 318 144 752	0.0252	98.05	94.01	46.36
Z_A1_3	62 550 528	9 445 129 728	61 973 662	9 094 604 280	0.0247	98.21	94.43	46.45
H_A1_1	49 428 280	7 463 670 280	48 909 500	7 178 503 469	0.0250	98.14	94.21	46.59
H_A1_2	44 645 648	6 741 492 848	44 195 576	6 520 913 549	0.0247	98.25	94.46	46.62
H_A1_3	51 897 454	7 836 515 554	51 361 446	7 520 260 169	0.0248	98.22	94.38	46.22
Z_A2_1	56 930 104	8 596 445 704	56 380 604	8 306 948 040	0.0252	98.02	93.92	46.66
Z_A2_2	53 412 762	8 065 327 062	52 949 916	7 838 951 682	0.0247	98.22	94.40	46.47
Z_A2_3	57 280 006	8 649 280 906	56 545 036	8 198 533 976	0.0252	98.03	93.98	46.57
H_A2_1	51 728 066	7 810 937 966	51 306 568	7 531 867 703	0.0250	98.14	94.13	46.57
H_A2_2	64 031 844	9 668 808 444	63 491 736	9 326 950 039	0.0248	98.22	94.35	46.26
H_A2_3	59 280 722	8 951 389 022	58 766 714	8 646 661 057	0.0248	98.20	94.34	46.54
Z_A3_1	52 526 848	7 931 554 048	51 938 048	7 634 886 704	0.0248	98.20	94.40	46.86
Z_A3_2	55 248 856	8 342 577 256	54 608 362	8 011 900 565	0.0249	98.17	94.31	46.77
Z_A3_3	53 670 962	8 104 315 262	53 022 918	7 738 357 730	0.0247	98.22	94.46	46.63
H_A3_1	60 832 178	9 185 658 878	60 192 462	8 814 536 731	0.0249	98.19	94.30	46.16
H_A3_2	53 626 590	8 097 615 090	53 058 904	7 839 563 407	0.0249	98.14	94.22	46.77
H_A3_3	60 487 788	9 133 655 988	59 940 364	8 766 180 348	0.0247	98.25	94.44	46.68
Mean value	55 647 145	8 402 718 979	55 083 136	8 083 593 249	0.0249	98.18	94.30	46.53

Q20, Q30 – quality scores; GC content – guanine-cytosine content

ples, including 28 989 known genes. Among these, the NR database had the highest number of annotated genes (27 916), while the KEGG database had the fewest annotated genes (10 403). Using a Venn diagram analysis, we observed that the NR database contained the highest number of unique genes (195) (Figure S1 in ESM).

Gene expression analysis. The RSEM software version 1.3.3 was employed for quantitative analysis of gene and novel transcript expression levels, with TPM as the quantitative metric. The distribution of gene expression levels across the 18 samples is depicted in Figure S2 in ESM. Based on gene expression levels, our analysis revealed that Group A1 had the highest number of specifically expressed genes (535), while Group C1 had the lowest (53) (Figure S3 in ESM). Correlation coefficient analysis of inter-gene expression levels showed good biological repeatability among the samples (Figure S4 in ESM). PCA indicated high similarity between biological replicates (Figure 2).

Analysis of DEGs. Based on gene read counts, differential gene analysis between groups was conducted using the DESeq2 software version 1.24.0 to identify genes with differential expression levels between the two groups. At 0 h post-inoculation, there were 3 370 DEGs between 'Ziguo' and 'Huangjinguo', including 2 470 up-regulated genes and 1 300 down-regulated genes. At 24 h post-inoculation, there were 4 464 DEGs between 'Ziguo 7' and 'Huangjinguo', with 2 507 up-regulated genes and 1 957 downregulated genes. At 48 h post-inoculation, there were 3 974 DEGs between 'Ziguo 7' and 'Huangjinguo', with 2 235 up-regulated genes and 1 739 downregulated genes (Figure 3A). Across all three time points, there were a total of 1 179 common DEGs (D gene set), accounting for 26.16% of the total. Considering that the DEGs at 0 hours between 'Ziguo 7' and 'Huangjinguo' were not induced by *Fusarium solani*, the DEGs induced by *Fusarium solani* were those common to 24 h and 48 h, excluding 0 h, with a total of 1 185 DEGs (E gene set) (Figure 3B, Table S2 in ESM).

GO functional annotation analysis. The GO database was used to perform functional classification analysis of the D and E gene sets. The results revealed that multicellular organismal process (biological process, BP) and structural molecule activity

https://doi.org/10.17221/161/2023-HORTSCI

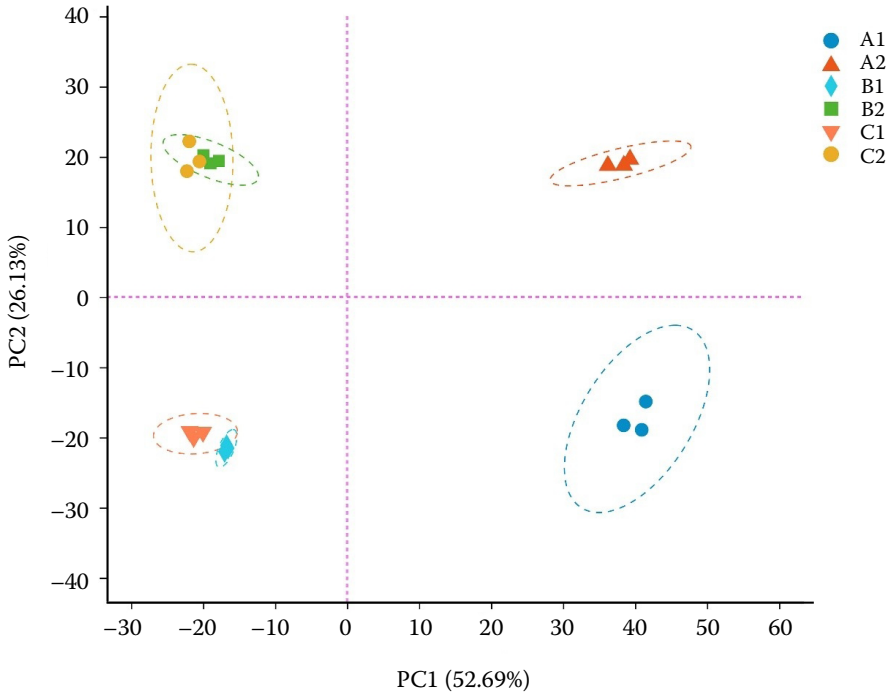

Figure 2. PCA analysis between 18 samples

The *X*-axis represents the contribution of principal component PC1 to the discriminative samples in the two-dimensional graph, the *Y*-axis represents the contribution of PC2 to the discriminative samples in the two-dimensional graph; PCA – principal component analysis; PC1, PC2 – principal components; A1–C2 – different comparative groups (gene sets)

(molecular function, MF) are specific GO terms for the D gene set, while reproductive process (BP) and extracellular region (cellular component, CC) were specific GO terms for the E gene set. Consequently, genes associated with the reproductive process (BP) and extracellular region (CC) may be linked to stem rot disease. The reproductive process (BP) GO term includes 20 genes (Table S3 in ESM), mainly associated with pollen development and flowering. The extracellular region (CC) GO term com-

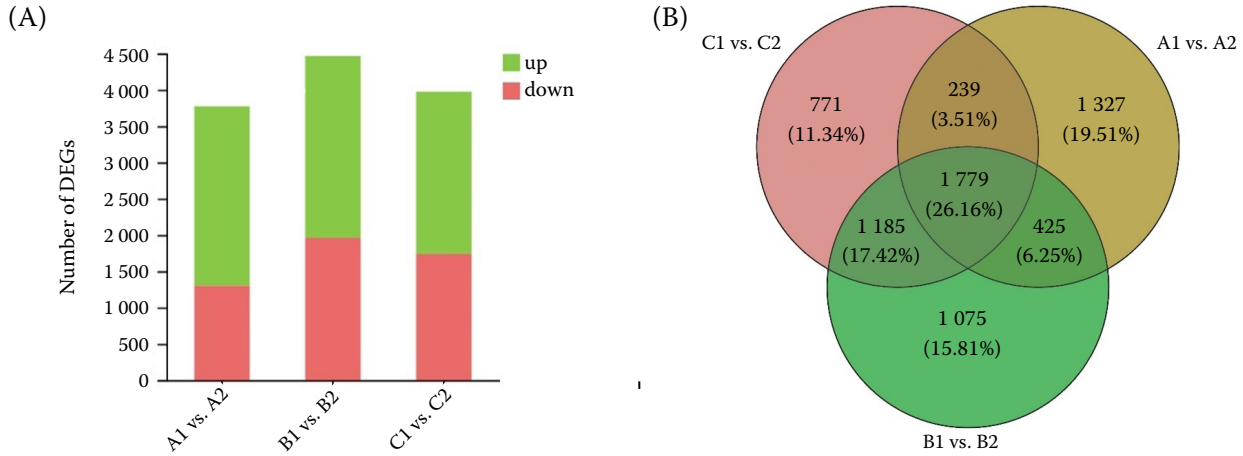

Figure 3. DEGs analysis during three stages of *Fusarium solani* infection in passion fruit

(A) DEGs – differentially expressed genes (green box – gene upregulation, red box – downregulation); (B) Different coloured circles represent different gene sets, and numerical values represent the number of shared and unique genes among different gene sets

A1–C2 – different comparative groups (gene sets)

https://doi.org/10.17221/161/2023-HORTSCI

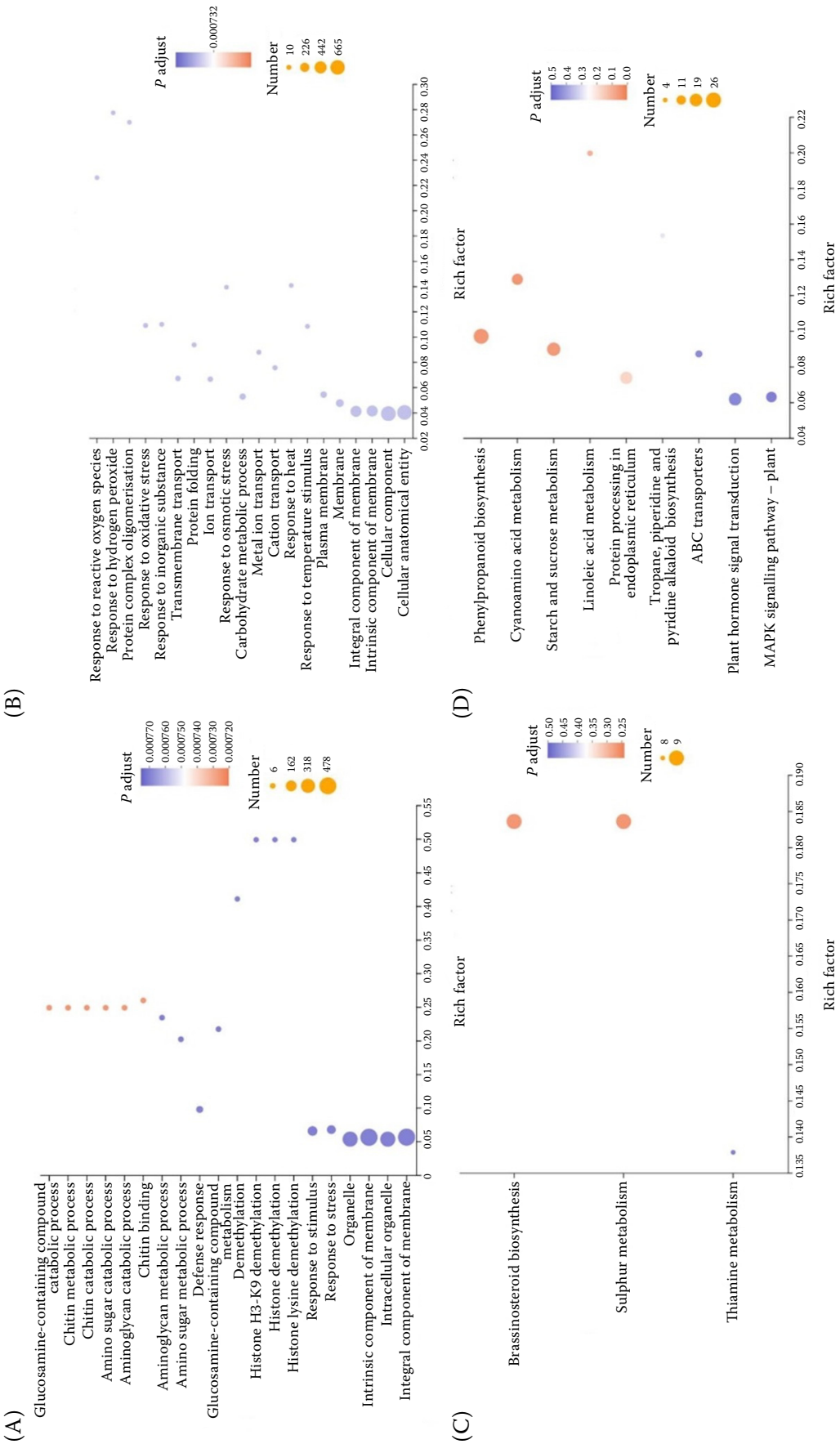

Figure 4. Functional enrichment analysis of DEGs (A) GO enrichment analysis of D gene set, (B) GO enrichment analysis of E gene set, (C) KEGG enrichment analysis of D gene set, (D) KEGG enrichment analysis of E gene set

The *X*-axis represents the Rich factor, the *Y*-axis represents terms, the size of the point represents the number of genes in this term or pathway, and the colour of the point corresponds to different *P* adjustment ranges

DEGs – differentially expressed genes; GO – Gene Ontology; KEGG – Kyoto Encyclopedia of Genes and Genomes

Horticultural Science (Prague), 52, 2025 (1): 67–80

https://doi.org/10.17221/161/2023-HORTSCI

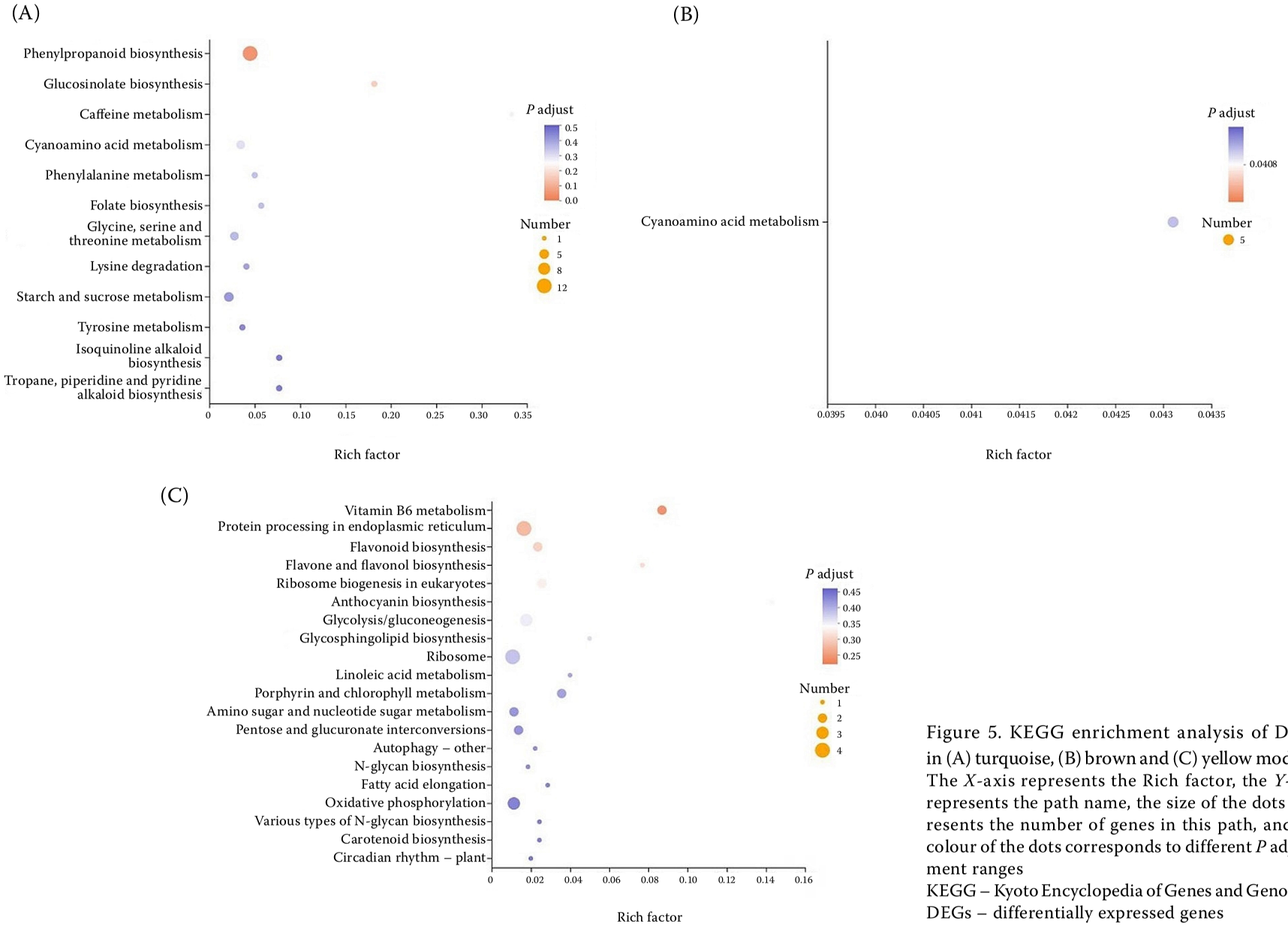

Figure 5. KEGG enrichment analysis of DEGs in (A) turquoise, (B) brown and (C) yellow modules
The *X*-axis represents the Rich factor, the *Y*-axis represents the path name, the size of the dots represents the number of genes in this path, and the colour of the dots corresponds to different *P* adjustment ranges
KEGG – Kyoto Encyclopedia of Genes and Genomes; DEGs – differentially expressed genes

https://doi.org/10.17221/161/2023-HORTSCI

prises 30 genes (Table S4 in ESM), primarily related to cell wall biogenesis, lignin catabolic processes, and response to oxidative stress.

GO and KEGG enrichment analysis. We used Goatools software to perform GO enrichment analysis on the genes within the D and E gene sets, aiming to identify the primary GO functions associated with these gene sets. The D gene set exhibited significant enrichment in functions related to glucosamine-containing compound catabolic process, chitin metabolic process, and chitin catabolic process (Figure 4A, Table S5 in ESM). On the other hand, the E gene set was mainly enriched in functions associated with response to reactive oxygen species (ROS), response to hydrogen peroxide, and protein complex oligomerisation (Figure 4B, Table S6 in ESM).

We used R package to perform KEGG pathway enrichment analysis on genes/transcripts within the D and E gene sets. The D gene set showed significant enrichment in pathways related to Brassinosteroid biosynthesis, Sulphur metabolism, and Thiamine metabolism (Figure 4C, Table S7 in ESM). On the other hand, the E gene set was primarily enriched in pathways such as phenylpropanoid biosynthesis, cyanoamino acid metabolism, and starch and sucrose metabolism (Figure 4D, Table S8 in ESM).

WGCNA analysis. The 1 185 DEGs (E gene set) were filtered based on the criteria TPM < 1 and coefficient of variation < 0.1, resulting in 954 DEGs, which were then used for constructing a weighted gene co-expression network. Correlation clustering analysis of the expression levels across the 18 samples showed good clustering between samples without any outliers (Figure S5 in ESM). We also conducted correlation analysis and clustering based on the TPM values of DEGs, where genes with high correlation were assigned to the same module. The clustering tree in the figure represents different branches of co-expressed gene modules, with different colours indicating distinct modules. A total of 5 modules were identified, and a gene co-expression network heatmap was generated (Figure S6 in ESM). The module significance (MS) values were obtained by calculating the average gene significance (GS) for all genes in each module. A higher MS value indicates greater importance, implying a stronger correlation with a specific phenotype feature (Table S9 in ESM). Correlation analysis between the trend of gene expression modules and disease resistance traits was performed. The screening criteria were set as a Pearson's correlation coefficient $r > 0.5$ and a significance $P < 0.05$. The turquoise module showed a positive correlation with disease resistance, while the brown and yellow modules showed a negative correlation with disease resistance (Table S10 in ESM). KEGG enrichment analysis was conducted on the DEGs within these three disease-related modules. The enriched pathways were mainly concentrated in phenylpropanoid biosynthesis (Figure 5A), flavonoid biosynthesis (Figure 5B), anthocyanin biosynthesis, and cyanoamino acid metabolism (Figure 5C).

The top 200 genes with the highest connectivity within the turquoise, brown, and yellow modules were selected for visualisation analysis (Figure 6). Among them, the top 10 hub genes with the highest connectivity were identified as follows: *ZX.08G0013660*, *ZX.01G0061280*, *ZX.01G0045360*, *ZX.02G0016900* (cinnamoyl-CoA reductase 1), *ZX.04G0033960*, *ZX.01G0086760*, *ZX.01G0015880*, *ZX.08G0027280*, *ZX.01G0104120*, and *ZX.08G0014080*. *ZX.08G0013660* is annotated as protein kinase binding, and conservative domain analysis showed that this gene contains a Leucine-rich repeat domain. *ZX.08G0013660* is located in the turquoise module, and there are 78 DEGs correlated with *ZX.08G0013660* (Figure 7A). *ZX.02G0016900* is annotated as dihydrokaempferol 4-reductase activity. *ZX.02G0016900* is also located in the turquoise module, and there are 98 DEGs correlated with *ZX.02G0016900* (Figure 7B).

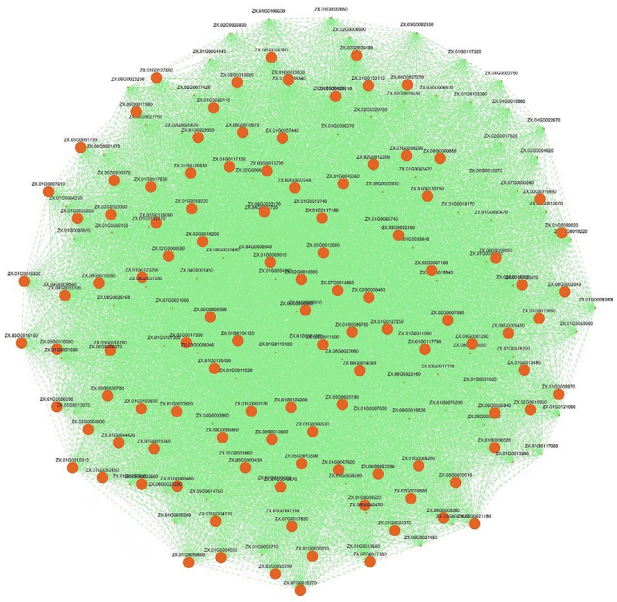

Figure 6. Co-expression network visualisation of turquoise, brown and yellow modules
In the visualisation graph, each node represents a gene

https://doi.org/10.17221/161/2023-HORTSCI

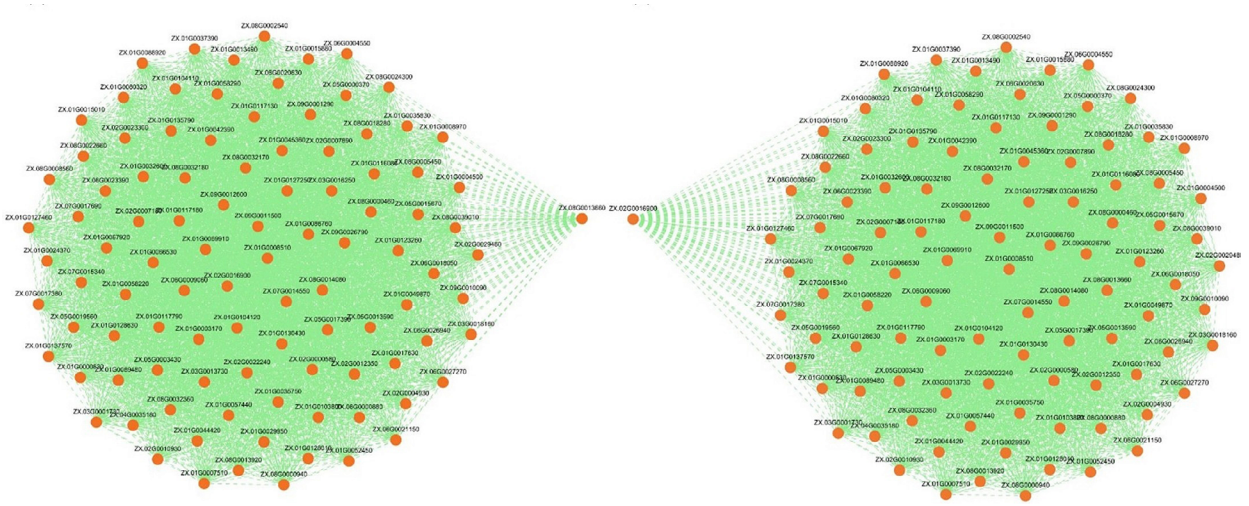

Figure 7. Putative hub genes of stem rot resistance in passion fruit (A) *ZX.08G0013660* and (B) *ZX.02G0016900*
In the visualisation graph, each node represents a gene

Candidate gene analysis and validation. In the GO and KEGG analyses, the functions and pathways related to response to ROS and phenylpropanoid biosynthesis showed the most significant enrichment. Previous studies have indicated the crucial roles of ROS and lignin in plant disease resistance (Dora et al. 2022). Lignin, a highly branched phenolic compound polymer, is activated by superoxide, hydrogen peroxide, hydroxyl radicals, and singlet oxygen systems, assembling into the final lignin polymer (Dora et al. 2022). Therefore, we selected the following genes for validation: *ZX.01G0011790*, *ZX.01G0021880*,

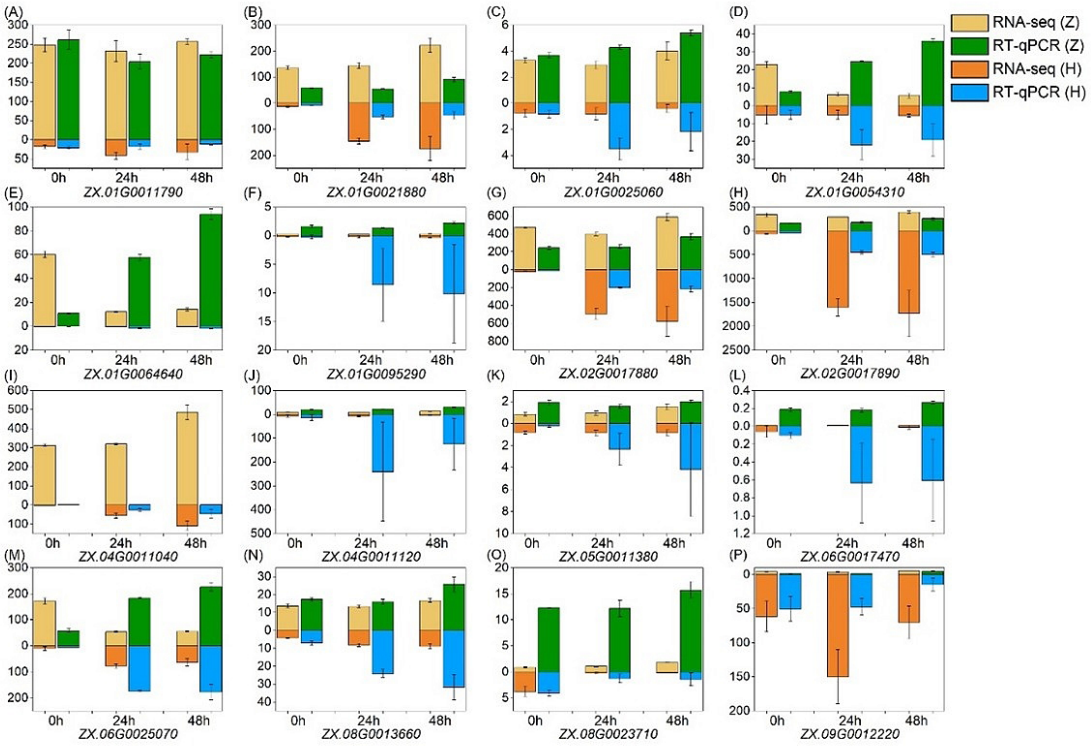

Figure 8. Using RT-qPCR to detect the expression levels of candidate genes in 'Huangjinguo' (H) and 'Ziguo 7' (Z)
RNA-seq – RNA-sequencing; RT-qPCR – reverse transcription quantitative real-time polymerase chain reaction

https://doi.org/10.17221/161/2023-HORTSCI

ZX.01G0025060, *ZX.01G0054310*, *ZX.01G0064640*, *ZX.01G0095290*, *ZX.02G0017880*, *ZX.02G0017890*, *ZX.04G0011040*, *ZX.04G0011120*, *ZX.05G0011380*, *ZX.06G0017470*, *ZX.06G0025070*, *ZX.08G0013660*, *ZX.08G0023710* and *ZX.09G0012220*. We downloaded coding sequences (CDS) of 18 genes from Majorbio (https://www.majorbio.com/web/www/index) and designed primers using Primer 5 software (Table S11 in ESM). After *Fusarium solani* infection of passion fruit 'Huangjinguo' and 'Ziguo 7', we analysed the expression of *EF-1α-2* and *EF1* and chose *EF-1α-2* as the reference gene for this study. The research results indicated that the expression trends of candidate genes in RT-qPCR and RNA-seq were consistent (Figure 8).

DISCUSSION

Fusarium solani, a fungus belonging to the phylum *Ascomycota*, order *Hypocreales*, and genus *Fusarium*, is widely distributed and contains numerous species that can infect a broad range of hosts (Coleman 2016). The hyphae of *Fusarium solani* are septate, colourless, and extensively branched. The conidia produced by *Fusarium solani* can be dispersed by rainwater, and infection occurs through wounds, with the infected sites continuously producing conidia for further re-infection. Previous studies have highlighted *Fusarium solani* as a major pathogen hindering the consecutive cultivation of apples, causing significant damage to apple root systems and inhibiting the normal growth of apple plants (Liu et al. 2023). In cucumber, *Fusarium solani* infection leads to roots and stems rot, and the affected vascular bundles exhibit a brown colour, eventually leading to wilting and death (Li et al. 2022). In tomato, *Fusarium solani* infection in the roots causes root rot disease, leading to a significant reduction in yield (Abd-Ellatif et al. 2022). When sweet potatoes are infected by *Fusarium solani*, the upper leaves exhibit yellowing and withering, and the underground storage roots become sunken and decayed, ultimately resulting in plant death (Xie et al. 2022). Currently, the primary method to control *Fusarium solani* is to use chemical agents, but this method, when used over the long term, not only pollutes the environment but also increases costs. Previous studies have indicated that utilising the inherent resistance of host plants is the most effective, economical, and environmentally friendly approach to control this disease (Deng et al. 2020). Therefore, identifying and characterising genes that confer resistance to *Fusarium solani* is of significant theoretical and practical importance for disease resistance breeding (Chitwood-Brown et al. 2021).

In this study, the resistance genes to stem rot in passion fruit were identified using RNA-seq technology. The results of GO functional enrichment analysis showed that the resistant genes were significantly correlated with ROS category. In plants, ROS plays a crucial role in sensing both biotic and abiotic stresses, integrating different environmental signals, and activating stress response networks, thus contributing to the establishment of defence mechanisms and the resilience of plants (Mittler et al. 2022). Among the 12 genes related to ROS, 11 genes were up-regulated in 'Huangjinguo'. Zhu et al. (2022) found that the β-carboline alkaloids in *Sophora flavescens* could inhibit *Fusarium solani* in ginseng roots by disrupting cell membranes and inducing the accumulation of ROS. The results of the study by Chen et al. (2019) indicate that *Harzianum* mould enhances cucumber's defence against *Fusarium solani* by regulating ROS and reactive nitrogen species (RNS) metabolism, redox balance, and energy flow in cucumber roots. Zhang et al. (2023) revealed a new mechanism in which tomato FolSrpk1 deacetylation regulates *Fusarium oxysporum* resistance in response to host ROS bursts. Miao et al. (2023) discovered that *CmWRKY6-1* negatively regulates resistance to *Fusarium oxysporum* and affects ROS and salicylic acid pathways. These studies collectively demonstrate the crucial role of ROS defence against *Fusarium* infection in plants.

The KEGG pathway enrichment analysis revealed associations with phenylpropanoid biosynthesis, a crucial pathway for secondary metabolites production in plants, particularly phenolic compounds. In higher plants, most phenolic substances originate from phenylalanine. *ZX.06G0025070*, *ZX.01G0064640*, *ZX.04G0011040*, *ZX.05G0011380* are annotated as lignin biosynthetic process (GO:0009809). Lignin is a highly branched polymeric compound derived from phenylpropanoid, composed of three different phenylpropanols: coniferyl alcohol, sinapyl alcohol, and *p*-coumaryl alcohol. Lignin plays a crucial role in plant defence by inhibiting the growth of pathogens. Singh et al. (2023) revealed that the effector *ArPEC25* negatively regulates lignin accumulation by targeting

https://doi.org/10.17221/161/2023-HORTSCI

the transcription factor CaβLIM1a, making chickpeas susceptible to necrotrophic pathogens. In rice, the expression of *OsPAL* family genes contributes to lignin synthesis, and a high lignin content is beneficial for enhancing rice resistance to diseases (Zhou et al. 2018). *OsPALs* positively regulate the biosynthesis and accumulation of salicylic acid and lignin, mediating rice resistance to brown planthopper (He et al. 2020). Tronchet et al. (2010) found that lignin plays a crucial role in disease resistance in *Arabidopsis*. Overexpression of *CmMYB19* in chrysanthemum enhances aphid tolerance by promoting lignin synthesis (Wang et al. 2017b). The cotton lignin synthesis gene *Gh4CL30* regulates lignification and phenolic content, playing a crucial role in resistance to *Fusarium wilt* (Xiong et al. 2021). *ZX.01G0054310*, *ZX.08G0023710*, *ZX.06G0017470*, *ZX.04G0011120*, *ZX.01G0095290*, *ZX.01G0025060*, and *ZX.01G0078630* are annotated as response to oxidative stress (GO:0006979). Previous studies have indicated that ROS induce the expression of callus synthesis genes and spatially restricted lignin deposition, contributing to physical barrier formation through cell wall reinforcement to impede invasion pathways (Dora et al. 2022). Therefore, both the ROS and phenylpropanoid biosynthesis pathways may be involved in the resistance response to stem rot in passion fruit.

WGCNA analysis indicates that *ZX.08G0013660* is associated with resistance to stem rot in passion fruit. By using the NCBI-Conserved Domains analysis tool, we predicted that *ZX.08G0013660* has four leucine-rich repeats. In plant cells, the nucleotide-binding leucine-rich repeat receptors (NLRs) directly or indirectly recognise effector proteins and trigger strong defence responses, which is potentially accompanied by the death of hypersensitive cells, providing resistance to diseases (Jacob et al. 2023). The wilt disease-resistant gene in tomato encodes an atypical leucine-rich repeat receptor-like protein whose function relies on SOBIR1 and SERK3/BAK1 (Catanzariti et al. 2017). Thapa et al. (2018) found that the response of leucine-rich repeat receptor-like kinases to pathogens is related to the *Fusarium* resistance in cereals. Coleman et al. (2021) demonstrated that leucine-rich repeat receptor-like kinase MIK2 is a crucial component of early immune responses to a fungal-derived elicitor. These studies collectively suggest that proteins containing leucine-rich repeat may contribute to enhancing resistance to stem rot in passion fruit.

CONCLUSION

In this study, we analysed the molecular basis underlying the difference in stem rot resistance between 'Huangjinguo' and 'Ziguo 7' using RNA-seq. Our findings reveal the involvement of the biological process response to ROS is involved in the stem rot resistance of passion fruit. At the same time, genes related to phenylpropanoid biosynthesis are significantly enriched in passion fruit's resistance against *Fusarium solani* infection. Lignin, a product of the oxidation polymerisation of three major lignin monomers, is synthesised in the cytoplasm through the general phenylpropanoid biosynthesis pathway and secreted to the cell wall. Once in the cell wall, these lignin monomers are activated by the superoxide, hydrogen peroxide, hydroxyl radicals, and singlet oxygen systems, assembling into the final lignin polymer. Furthermore, there was a significant difference in the expression level of leucine-rich repeat protein genes between 'Huangjinguo' and 'Ziguo 7'. Collectively, these results underscore the importance of ROS, the phenylpropanoid biosynthesis pathway and leucine-rich repeat domain proteins in conferring stem rot resistance in passion fruit.

REFERENCES

Abd-Ellatif S., Ibrahim A.A., Safhi F.A., Abdel Razik E.S., Kabeil S., Aloufi S., Alyamani A.A., Basuoni M.M., Alshamrani S.M., Elshafie H.S. (2022): Green synthesised of *Thymus vulgaris* chitosan nanoparticles induce relative WRKY-Genes expression in *Solanum lycopersicum* against *Fusarium solani*, the causal agent of root rot disease. Plants, 11: 3129.

Bai H., Si H., Zang J., Pang X., Yu L., Cao H., Xing J., Zhang K., Dong J. (2021): Comparative proteomic analysis of the defense response to *Gibberella* stalk rot in maise and reveals that ZmWRKY83 is involved in plant disease resistance. Frontiers in Plant Science, 12: 694973.

Belisário R., Robertson A.E., Vaillancourt L.J. (2022): Maize anthracnose stalk rot in the genomic era. Plant Disease, 106: 2281–2298.

Catanzariti A.M., Do H.T., Bru P., De Sain M., Thatcher L.F., Rep M., Jones D.A. (2017): The tomato *I* gene for Fusarium wilt resistance encodes an atypical leucine-rich repeat receptor-like protein whose function is nevertheless dependent on SOBIR1 and SERK3/BAK1. The Plant Journal, 89: 1195–1209.

https://doi.org/10.17221/161/2023-HORTSCI

Chen Q., Song J., Du W.P., Xu L.Y., Jiang Y., Zhang J., Xiang X.L., Yu G.R. (2017): Identification, mapping, and molecular marker development for *Rgsr8.1*: A new quantitative trait locus conferring resistance to *Gibberella* stalk rot in maise (*Zea mays* L.). Frontiers in Plant Science, 8: 1355.

Chen S.C., Ren J.J., Zhao H.J., Wang X.L., Wang T.H., Jin S.D., Wang Z.H., Li C.Y., Liu A.R., Lin X.M., Ahammed G.J.. (2019): *Trichoderma harzianum* improves defense against *Fusarium oxysporum* by regulating ROS and RNS metabolism, redox balance, and energy flow in cucumber roots. Phytopathology, 109: 972–982.

Chitwood-Brown J., Vallad G.E., Lee T.G., Hutton S.F. (2021): Breeding for resistance to *Fusarium wilt* of tomato: A review. Genes (Basel), 12: 1673.

Coleman J.J. (2016): The *Fusarium solani* species complex: Ubiquitous pathogens of agricultural importance. Molecular Plant Pathology, 17: 146–158.

Coleman A.D., Maroschek J., Raasch L., Takken F., Ranf S., Hückelhoven R. (2021): The Arabidopsis leucine-rich repeat receptor-like kinase MIK2 is a crucial component of early immune responses to a fungal-derived elicitor. New Phytologist, 229: 3453–3466.

Deng Y., Ning Y., Yang D.L., Zhai K., Wang G.L., He Z. (2020): Molecular basis of disease resistance and perspectives on breeding strategies for resistance improvement in crops. Molecular Plant, 13: 1402–1419.

Dora S., Terrett O.M., Sánchez-Rodríguez C. (2022): Plant-microbe interactions in the apoplast: Communication at the plant cell wall. The Plant Cell, 34: 1532–1550.

Du Q., Yang X., Zhang J., Zhong X., Kim K.S., Yang J., Xing G., Li X., Jiang Z., Li Q., Dong Y., Pan H. (2018): Over-expression of the *Pseudomonas syringae* harpin-encoding gene *hrpZm* confers enhanced tolerance to *Phytophthora* root and stem rot in transgenic soybean. Transgenic Research, 27: 277–288.

Du F., Tao Y., Ma C., Zhu M., Guo C., Xu M. (2023): Effects of the quantitative trait locus *qPss3* on inhibition of photoperiod sensitivity and resistance to stalk rot disease in maise. Theoretical and Applied Genetics, 136: 126.

Duan C., Song F., Sun S., Guo C., Zhu Z., Wang X. (2019): Characterisation and molecular mapping of two novel genes resistant to *Pythium* stalk rot in maise. Phytopathology, 109: 804–809.

Funnell-Harris D.L., Sattler S.E., O'Neill P.M., Gries T., Tetreault H.M., Clemente T.E. (2019): Response of sorghum enhanced in monolignol biosynthesis to stalk rot pathogens. Plant Disease, 103: 2277–2287.

He J., Liu Y., Yuan D., Duan M., Liu Y., Shen Z., Yang C., Qiu Z., Liu D., Wen P., Huang J., Fan D., Xiao S., Xin Y., Chen X., Jiang L., Wang H., Yuan L., Wan J. (2020): An R2R3 MYB transcription factor confers brown planthopper resistance by regulating the phenylalanine ammonia-lyase pathway in rice. Proceedings of the National Academy of Sciences, 117: 271–277.

Jacob P., Hige J., Dangl J.L. (2023): Is localised acquired resistance the mechanism for effector-triggered disease resistance in plants? Nature Plants, 9: 1184–1190.

Li J., Luan Q., Han J., Chen C., Ren Z. (2022): *CsMYB60* confers enhanced resistance to *Fusarium solani* by increasing proanthocyanidin biosynthesis in cucumber. Phytopathology, 112: 588–594.

Liu Y., Guo Y., Ma C., Zhang D., Wang C., Yang Q. (2016): Transcriptome analysis of maise resistance to *Fusarium graminearum*. BMC Genomics, 17: 477.

Liu Y., Liu Q., Li X., Zhang Z., Ai S., Liu C., Ma F., Li C. (2023): *MdERF114* enhances the resistance of apple roots to *Fusarium solani* by regulating the transcription of MdPRX63. Plant Physiology, 192: 2015–2029.

Ma C., Ma X., Yao L., Liu Y., Du F., Yang X., Xu M. (2017): *qRfg3*, a novel quantitative resistance locus against *Gibberella* stalk rot in maise. Theoretical and Applied Genetics, 130: 1723–1734.

Ma P., Liu E., Zhang Z., Li T., Zhou Z., Yao W., Chen J., Wu J., Xu Y., Zhang H. (2023): Genetic variation in *ZmWAX2* confers maise resistance to *Fusarium verticillioides*. Plant Biotechnology Journal, 21: 1812–1826.

Miao W., Xiao X., Wang Y., Ge L., Yang Y., Liu Y., Liao Y., Guan Z., Chen S., Fang W., Chen F., Zhao S. (2023): CmWRKY6-1-CmWRKY15-like transcriptional cascade negatively regulates the resistance to *Fusarium oxysporum* infection in *Chrysanthemum morifolium*. Horticulture Research, 10: uhad101.

Mittler R., Zandalinas S.I., Fichman Y., Van Breusegem F. (2022): Reactive oxygen species signalling in plant stress responses. Nature Reviews Molecular Cell Biology, 23: 663–679.

Singh S.K., Shree A., Verma S., Singh K., Kumar K., Srivastava V., Singh R., Saxena S., Singh A.P., Pandey A., Verma P.K. (2023): The nuclear effector ArPEC25 from the necrotrophic fungus *Ascochyta rabiei* targets the chickpea transcription factor CaβLIM1a and negatively modulates lignin biosynthesis, increasing host susceptibility. The Plant Cell, 35: 1134–1159.

Thapa G., Gunupuru L.R., Hehir J.G., Kahla A., Mullins E., Doohan F.M. (2018): A pathogen-responsive leucine rich receptor like kinase contributes to *Fusarium* resistance in cereals. Frontiers in Plant Science, 9: 867.

Tronchet M., Balagué C., Kroj T., Jouanin L., Roby D. (2010): Cinnamyl alcohol dehydrogenases-C and D, key enzymes in lignin biosynthesis, play an essential role in disease resistance in Arabidopsis. Molecular Plant Pathology, 11: 83–92.

https://doi.org/10.17221/161/2023-HORTSCI

Wang C., Yang Q., Wang W., Li Y., Guo Y., Zhang D., Ma X., Song W., Zhao J., Xu M. (2017a): A transposon-directed epigenetic change in *ZmCCT* underlies quantitative resistance to *Gibberella* stalk rot in maise. New Phytologist, 215: 1503–1515.

Wang Y., Sheng L., Zhang H., Du X., An C., Xia X., Chen F., Jiang J., Chen S. (2017b): *CmMYB19* over-expression improves aphid tolerance in chrysanthemum by promoting lignin synthesis. International Journal of Molecular Sciences, 18: 619.

Wu Y., Tian Q., Huang W., Liu J., Xia X., Yang X., Mou H. (2020): Identification and evaluation of reference genes for quantitative real-time PCR analysis in *Passiflora edulis* under stem rot condition. Molecular Biology Reports, 47: 2951–2962.

Wu Y., Huang W., Tian Q., Liu J., Xia X., Yang X., Mou H. (2021): Comparative transcriptomic analysis reveals the cold acclimation during chilling stress in sensitive and resistant passion fruit (*Passiflora edulis*) cultivars. PeerJ, 9: e10977.

Xie S.Y., Ma T., Zhao N., Zhang X., Fang B., Huang L. (2022): Whole-genome sequencing and comparative genome analysis of *Fusarium solani-melongenae* causing *Fusarium* root and stem rot in sweetpotatoes. Microbiology Spectrum, 10: e0068322.

Xiong X.P., Sun S.C., Zhu Q.H., Zhang X.Y., Li Y.J., Liu F., Xue F., Sun J. (2021): The cotton lignin biosynthetic gene *Gh4CL30* regulates lignification and phenolic content and contributes to Verticillium wilt resistance. Molecular Plant-Microbe Interactions, 34: 240–254.

Ye J., Guo Y., Zhang D., Zhang N., Wang C., Xu M. (2013): Cytological and molecular characterisation of quantitative trait locus *qRfg1*, which confers resistance to *Gibberella* stalk rot in maise. Molecular Plant-Microbe Interactions, 26: 1417–1428.

Ye J., Zhong T., Zhang D., Ma C., Wang L., Yao L., Zhang Q., Zhu M., Xu M. (2019): The auxin-regulated protein ZmAuxRP1 coordinates the balance between root growth and stalk rot disease resistance in maise. Molecular Plant, 12: 360–373.

Zhang N., Lv F., Qiu F., Han D., Xu Y., Liang W. (2023): Pathogenic fungi neutralise plant-derived ROS via Srpk1 deacetylation. The EMBO Journal, 42: e112634.

Zhao M., Fan H., Tu Z., Cai G., Zhang L., Li A., Xu M. (2022): Stable reference gene selection for quantitative real-time PCR normalisation in Passion fruit (*Passiflora edulis* Sims.). Molecular Biology Reports, 49: 5985–5995.

Zhou X., Liao H., Chern M., Yin J., Chen Y., Wang J., Zhu X., Chen Z., Yuan C., Zhao W., Wang J., Li W., He M., Ma B., Wang J., Qin P., Chen W., Wang Y., Liu J., Qian Y., Wang W., Wu X., Li P., Zhu L., Li S., Ronald P.C., Chen X. (2018): Loss of function of a rice TPR-domain RNA-binding protein confers broad-spectrum disease resistance. Proceedings of the National Academy of Sciences, 115: 3174–3179.

Zhu Z., Zhao S., Wang C. (2022): β-carboline alkaloids from *Peganum harmala* inhibit *Fusarium oxysporum* from *Codonopsis radix* through damaging the cell membrane and inducing ROS accumulation. Pathogens, 11: 1341.

Received: December 7, 2023
Accepted: July 15, 2024
Published online: March 19, 2025